

## Si(001) Dimer Structure Observed with Scanning Tunneling Microscopy

R. M. Tromp, R. J. Hamers, and J. E. Demuth

*IBM Thomas J. Watson Research Center, Yorktown Heights, New York 10598*

(Received 16 July 1985)

Scanning tunneling microscopy has been used to determine the atomic structure of the clean Si(001) surface. The basic structural unit of the reconstruction has been resolved with a lateral resolution of  $\sim 3$  Å. Buckled and nonbuckled dimers appear to be present in roughly equal amounts, indicating that they have nearly the same energy. The presence of atomic-scale defects is discussed.

PACS numbers: 68.20.+t, 61.16.-d, 61.70.-r, 68.40.+e

In recent years the clean Si(001) surface has been the focus of many experimental and theoretical studies.<sup>1,2</sup> In spite of all these efforts the atomic structure of this technologically important surface remains in doubt. In the bulklike terminated surface each of the first-layer atoms is bonded to two atoms in the second layer, leaving two dangling bonds on each surface atom. The high energy associated with these dangling bonds is lowered by surface reconstruction. In most low-energy electron-diffraction (LEED) experiments on this surface a  $(2 \times 1)$  diffraction pattern is observed, indicating a doubling of the surface periodicity in one direction.<sup>3</sup> In some studies, however, a  $c(4 \times 2)$  pattern was observed,<sup>4,5</sup> while atom diffraction studies showed the presence of  $(2 \times 1)$ ,  $c(4 \times 2)$ , and  $(2 \times 2)$  domains.<sup>6</sup> Of the structural models proposed for this surface the dimer model<sup>7</sup> which appears to explain most of the experimental results is most widely supported. Other models are the conjugated-chain model by Seiwatz,<sup>8</sup> later elaborated on by Chadi,<sup>9</sup> and the missing-row models discussed by Harrison<sup>10</sup> and by Poppendieck, Gnoc, and Webb.<sup>5</sup> The dimer model was recently questioned by Pandey,<sup>11</sup> who proposed that—in addition to the dimers—the surface should have a rather large number of defects. The nature of these defects will be discussed later. In Northrup's recent model<sup>12</sup> dimers form a  $(2 \times 1)$  structure in the second layer of the crystal. On top of these the atoms in the first layer form chains, in analogy to the chains found on the cleaved Si(111)- $(2 \times 1)$  surface.<sup>13</sup> In his self-consistent pseudopotential calculations, Northrup found this dimer-chain model to have a slightly lower energy than the dimer model,<sup>12</sup> even though the structure is very different.

Given the small energy differences calculated for various models and the observation of different diffraction patterns in LEED and atom-diffraction experiments, it is reasonable that the clean Si(001) surface may exhibit more than one reconstruction, as for example observed on epitaxial Ge on Si(111).<sup>14</sup> This occurrence of different reconstructions simultaneously on the same surface complicates the interpretation of experimental results that average over a large surface area and may explain why a definitive surface structure

determination has not been possible.

In this Letter we present the first study of the Si(001) surface with extremely high lateral resolution ( $\sim 3$  Å), using scanning tunneling microscopy (STM). At present, STM seems to be the only technique that may resolve the uncertainties discussed above. The principles of STM have been first explained and fully exploited in the pioneering work of Binnig *et al.*<sup>15</sup> A fine metal tip mounted on three orthogonal piezoelectric drives is brought very close ( $\sim 10$  Å) to the surface under investigation. When a bias is applied between tip and sample, electrons can tunnel from one to the other. When the tip is scanned along the surface by means of the two piezoelectric drives parallel to the surface ( $X$  and  $Y$ ), the tunneling current tends to change because of variations in work function and electron density and because of surface corrugations. In the experiment the tunneling current is kept constant in a feedback circuit by adjustment of the distance between tip and sample with the third piezoelectric drive ( $Z$ ), normal to the surface. When the  $X$  and  $Y$  drives are being scanned, the voltage applied to the  $Z$  drive is a measure of electronic and topological changes along the scans. The results thus obtained can be presented as an image of the scanned area. In our experiment the calibration of the piezoelectrical drives was determined from topographs of the Si(111)- $(7 \times 7)$  surface where spacings are well known.<sup>16</sup>

The microscope used in this study<sup>16</sup> does not have a piezoelectric walker ("louse") as in most other microscopes.<sup>15</sup> Instead, all translations of the sample are accomplished with one rotary motion feedthrough. The sample is brought down onto a foot close to the tip. When the sample is lowered further it pivots on the foot and can be brought smoothly into tunneling distance. The mechanical contact between sample and foot provides efficient vibration damping, posing less stringent restrictions on the physical environment of the experiment. When the sample is moved far away from the tip and off the foot, it flips up. In this position it can be heated by passing a direct current through the sample.  $n$ -type Si samples ( $5 \times 15 \times 0.3$  mm<sup>3</sup>,  $0.1 \Omega \cdot \text{cm}$ , P doped) were cut from a (001)

wafer, rinsed in ethanol, and mounted on a Ta support. The samples were held by steel clips separated from the sample with Si spacers cut from the same wafer. After system bakeout the sample was thoroughly outgassed at 600 °C until the background pressure was restored to its initial value ( $\sim 10^{-10}$  Torr). A clean surface was obtained by heating the sample to 1050 °C during 2 min, followed by a gradual cooldown during 3–4 min. In order to reduce thermal drifts the sample holder assembly was then allowed to cool for 3 h. The microscope chamber has no other surface analytical tools, but when the cleaning procedure was used in another chamber with a sample holder of identical construction sharp ( $2 \times 1$ ) LEED patterns were obtained routinely.

Surface topographs were recorded with a bias of  $-2$  V applied to the sample while the W tip was grounded and with a tunneling current of 1 nA. Typical scanning speeds were 20–40 Å/s. Data accumulation was controlled by an IBM PC/XT personal computer. Image analysis was performed on an off-line IBM 3081 computer.

Figure 1 shows two gray-scale topographs of the clean Si(001) surface. The bar indicates a distance of 25 Å. In these images surface protrusions are white, depressions are black. The total gray-scale range corresponds to a displacement of 1 Å of the Z drive. The images have been corrected for drift in the microscope

occurring during the scans. By linear transformation lines A and B [Fig. 1(a)] were made to intersect at an angle of 90°. That these lines indeed intersect at a 90° angle has been verified in the observation of an atomic step where the entire reconstruction pattern rotates over an angle of 90° (not shown). Although the two topographs shown here were obtained on one sample, very similar results have been obtained on several Si(001) crystals. The most striking feature in Fig. 1 consists of rows of oblong protrusions. These rows have been labeled from 1a to 19a in Fig. 1(a) and from 1b to 19b in Fig. 1(b). The rows are separated by 7.7 Å, while the distance between the protrusions in the rows as, for instance, in rows 11a and 13a, is half this distance, approximately 3.8 Å. Figure 2(a) shows the corrugation as measured along line A in Fig. 1(a), where left and right in Fig. 1(a) correspond with left and right in Fig. 2(a). The horizontal scale in Fig. 2(a) is given in units of  $a_0\sqrt{2}$ , twice the lattice constant of the unreconstructed surface ( $a_0 = 5.43$  Å). The small corrugation along this direction, only 0.15 Å, has the same periodicity as the unreconstructed surface and suggests a resolution of about 3 Å. This represents the highest lateral resolution achieved to date on a semiconductor surface and is consistent with estimates by Tersoff and Hamann.<sup>17</sup>

Row 11a is one of the few rows that do not have any additional features. In the adjacent row, 12a, a surface

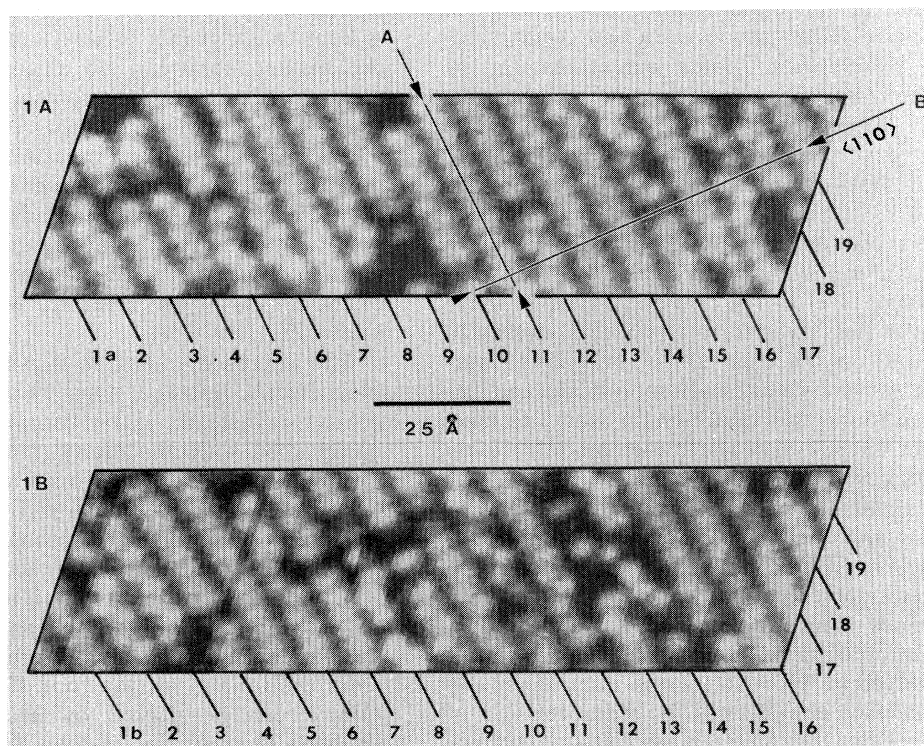


FIG. 1. Gray-scale topographs of the Si(001) surface. For a discussion see text.

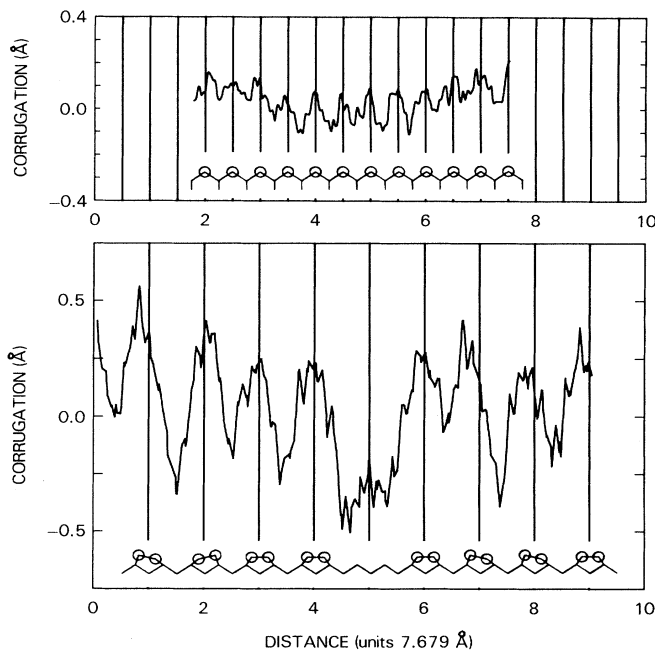


FIG. 2. Corrugation measured along (a) line A and (b) line B in Fig. 1(a). The horizontal axis is in units of  $7.679 \text{ \AA}$  ( $a_0\sqrt{2}$ ), twice the lattice constant of the unreconstructed surface. Left and right corresponds with left and right in Fig. 1(a). The underlying atomic structure is indicated schematically.

defect consisting of a missing protrusion can be observed near the center. Further down the row a zigzag pattern is found. These two features also occur in many other places in Fig. 1. Figure 2(b) shows the corrugation perpendicular to the rows, along line B in Fig. 1(a). This particular line passes through a missing protrusion (15a), several zigzags (11a, 12a, 17a, and 18a), and nonzigzag rows. Again, the horizontal scale is in units of  $a_0\sqrt{2}$  and the corrugation has just this periodicity, with a peak-to-peak amplitude of  $0.4\text{--}0.7 \text{ \AA}$ . The defect in row 15a is slightly deeper. In rows 11a, 12a, 17a, and 18a the asymmetry of the corrugation due to the zigzag pattern is apparent.

The topographs presented here are most easily explained by a dimer model. The dimers may be parallel to the surface (as they are in about half of the rows) or they may be buckled. Alternation of the buckling along a row gives rise to the zigzag pattern. The defect in row 15a is interpreted as a missing dimer, very similar to the  $\pi$ -bonded defect proposed by Pandey.<sup>11</sup> In Fig. 2(a) the dimers are viewed end on, with a periodicity of  $a_0/\sqrt{2}$ . In Fig. 2(b) the dimers give rise to periodicity doubling and asymmetries in the corrugation as indicated.

We now turn to the local symmetry of the surface. In many places, where the dimers are not buckled, the periodicity is  $(2 \times 1)$ , but in other places different sym-

metries are observed. For example, in the upper part of rows 14a and 15a, the symmetry is  $p(2 \times 2)$ , while in the lower part of rows 2b and 3b it is  $c(4 \times 2)$ . Most of the rows of buckled dimers, however, do not exhibit a particular relation to the adjacent rows, often because these are not buckled.

We do not observe any of the chainlike structures proposed by Seiwatz<sup>8</sup> and Northrup.<sup>12</sup> Since the distance between features in these models is only  $2.35 \text{ \AA}$ , while the resolution of the microscope is  $\sim 3 \text{ \AA}$ , these chainlike structures would give rise to continuous bandlike protrusions, as opposed to the well-resolved maxima in Figs. 1 and 2. The data also seem to exclude missing-row models as discussed by Harrison<sup>10</sup> and by Poppendieck, Gnoc, and Webb.<sup>5</sup> In these models the surface layer does not contain dimers, but rows of single atoms, separated by  $a_0\sqrt{2}$  in one direction and  $a_0/\sqrt{2}$  in the other. The removal of rows of atoms exposes deeper layers to the vacuum and one would expect a very large corrugation along the direction of periodicity doubling, which is not observed. Furthermore it would be difficult to explain symmetries other than  $(2 \times 1)$  with a missing-row model. Although the model by Poppendieck, Gnoc, and Webb has  $c(4 \times 2)$  symmetry,<sup>5</sup> the periodicity doubling along the rows is caused by distortions in the second and third layer, which would not be observed by STM. By removing every second atom in each atomic row in an alternating fashion one obtains a  $c(2 \times 2)$  structure, which is not observed. Thus, missing-row models are expected to give very large corrugation along line B, and a nondoubled periodicity along line A. The experimental results are in disagreement with these expectations.

A surprising result of our measurements is that the dimers sometimes do and other times do not buckle. Buckled dimers have been proposed in a number of theoretical studies including cluster,<sup>18</sup> empirical tight-binding,<sup>19</sup> and self-consistent pseudopotential calculations.<sup>20</sup> Pandey<sup>11</sup> has shown that buckling involving charge transfer to the top atom is an artifact of tight-binding calculations. He found that the nonbuckled dimer is energetically most favorable, but buckling up to a dimer tilt angle of  $10^\circ$  did not increase the total energy significantly.<sup>11</sup> These calculations were performed in a  $(2 \times 1)$  unit cell where all dimers in a row buckle in the same direction. Our results show that the buckling direction switches from dimer to dimer along a row, in local  $(2 \times 2)$  symmetry. It appears that in this configuration the energy at relatively large buckling angles is still comparable to that of the symmetric dimers, possibly because there is less bond-angle strain in a  $(2 \times 2)$  arrangement of buckled dimers than in a  $(2 \times 1)$  buckled dimer cell.

The missing dimer, as in rows 12a and 15a, occurs rather often. Pandey proposed this defect on the basis

of theoretical considerations.<sup>11</sup> When a dimer is missing, four broken bonds are present in the second layer. Dimerization in the second layer in a direction parallel to the rows eliminates these broken bonds. This stabilization is partially offset by the elastic strain induced by the dimerization. However, if the defects are sufficiently far apart so that their elastic strain fields do not overlap, the net energy is lowered. Larger defects, observed in the upper left-hand and lower right-hand corners of Fig. 1(a), appear to be of a different nature. Line scans like the ones shown in Fig. 2 reveal that the larger defects as in rows 8a-9a are deeper than the single defect in row 15a. The black area in 8a-9a is  $\sim 1.1$  Å below the top of the dimers, giving very clear evidence that the second layer is exposed to the vacuum. In a symmetric-dimer model the dimer atoms are  $\sim 1.2$  Å above the atoms in the second layer.

In this Letter we have presented the first STM study of the atomic structure of the clean Si(001) surface. We have established the basic nature of the reconstruction: Both buckled and nonbuckled dimers are present, in roughly equal proportions, suggesting that their energies are nearly degenerate. Defects occur in rather large numbers. Some of these defects are similar to the  $\pi$ -bonded defect proposed by Pandey. Although it is likely that the ratio of buckled to nonbuckled dimers and the density of single and multiple missing-dimer defects depend on the exact preparation of the clean surface and on remaining surface impurities, there is little doubt that the features observed in Fig. 1 are present on any Si(001)-(2 $\times$ 1) surface. We have repeated our experiments on several samples with essentially the same results. We did find, however, that prolonged annealing at 1050–1100 °C results in considerable surface roughness.

The authors thank Peter Schroer for his assistance in

setting up the electronics and computer interface, and Bill Thompson for the LEED experiments. This work is supported in part by the U.S. Office of Naval Research.

<sup>1</sup>D. E. Eastman, *J. Vac. Sci. Technol.* **17**, 492 (1980).

<sup>2</sup>W. Monch, *Surf. Sci.* **86**, 672 (1979).

<sup>3</sup>R. E. Schlier and H. E. Farnsworth, in *Semiconductor Surface Physics*, edited by R. H. Kingston (Univ. of Pennsylvania Press, Philadelphia, 1957), p. 3.

<sup>4</sup>J. J. Lander and J. Morrison, *J. Appl. Phys.* **33**, 2089 (1962), and *J. Chem. Phys.* **37**, 729 (1962).

<sup>5</sup>T. D. Poppendieck, T. C. Gnoc, and M. B. Webb, *Surf. Sci.* **75**, 287 (1978).

<sup>6</sup>M. J. Cardillo and G. E. Becker, *Phys. Rev. Lett.* **40**, 1148 (1978), and *Phys. Rev. B* **21**, 1497 (1980).

<sup>7</sup>J. D. Levine, *Surf. Sci.* **34**, 90 (1973).

<sup>8</sup>R. Seiwatz, *Surf. Sci.* **2**, 473 (1963).

<sup>9</sup>D. J. Chadi, *J. Vac. Sci. Technol.* **16**, 1290 (1979).

<sup>10</sup>W. A. Harrison, *Surf. Sci.* **55**, 1 (1976).

<sup>11</sup>K. C. Pandey, in *Proceedings of the Seventeenth International Conference on the Physics of Semiconductors*, edited by D. J. Chadi and W. A. Harrison (Springer-Verlag, New York, 1985), p. 55.

<sup>12</sup>J. Northrup, *Phys. Rev. Lett.* **54**, 815 (1985).

<sup>13</sup>K. C. Pandey, *Phys. Rev. Lett.* **47**, 1913 (1981).

<sup>14</sup>R. S. Becker, J. A. Golovchenko, and B. S. Swartzentruber, *Phys. Rev. Lett.* **54**, 2678 (1985).

<sup>15</sup>G. Binnig, H. Rohrer, Ch. Gerber, and E. Weibel, *Phys. Rev. Lett.* **49**, 57 (1982), and **50**, 120 (1983).

<sup>16</sup>J. E. Demuth, R. Hamers, R. M. Tromp, and M. Weland, to be published.

<sup>17</sup>J. Tersoff and D. Hamann, *Phys. Rev. B* **31**, 805 (1985).

<sup>18</sup>W. S. Verwoerd, *Surf. Sci.* **99**, 581 (1980).

<sup>19</sup>D. J. Chadi, *Phys. Rev. Lett.* **43**, 43 (1979).

<sup>20</sup>M. T. Yin and M. L. Cohen, *Phys. Rev. B* **24**, 2303 (1981).

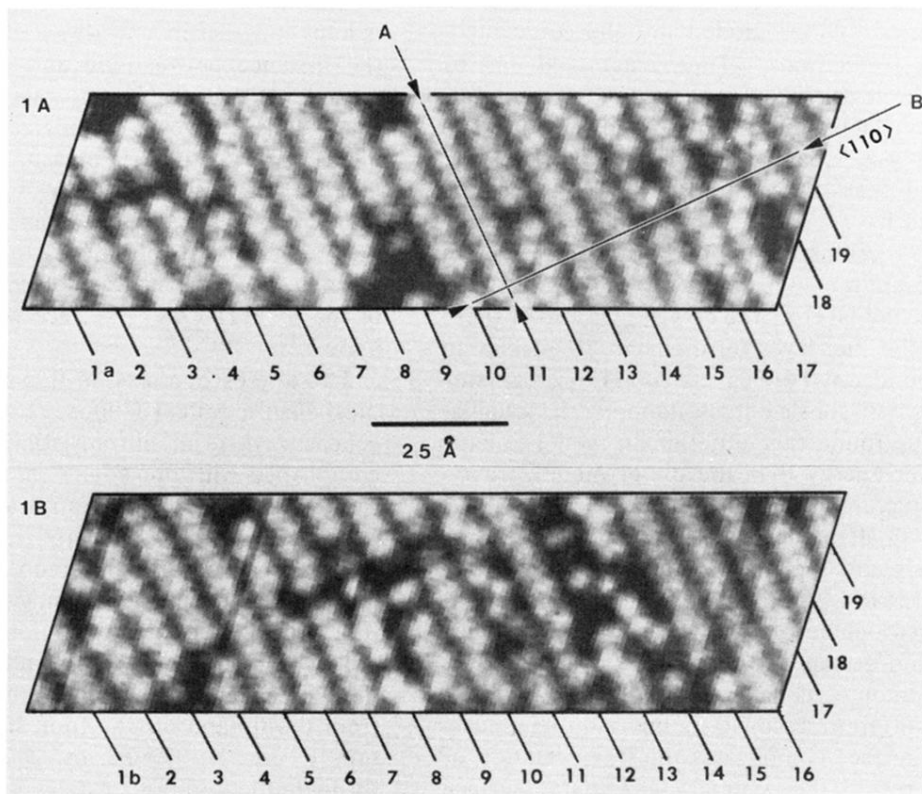


FIG. 1. Gray-scale topographs of the Si(001) surface. For a discussion see text.